J. Fluid Mech. (1977), *vol.* 81, *part* 3, *pp.* 401–419
Printed in Great Britain

The steady movement of a liquid meniscus in a capillary tube

By C. HUH† AND S. G. MASON
Department of Chemistry, McGill University, Montreal, Canada

(Received 5 June 1975 and in revised form 8 April 1976)

The steady movement of a liquid meniscus in a circular capillary tube has been examined theoretically for dynamic contact angles close to 90° with minute slippage of the liquid on the solid, thus relaxing the conventional no-slip boundary condition. The resulting flow field does not produce an unbounded force at the contact line, contrary to that with the no-slip condition. The interfacial velocity, wall stress, fluid pressure and the meniscus shape are calculated, and the significance of dynamic contact-angle measurements is discussed. A modified version of the classical Washburn equation which takes account of the meniscus also reveals the importance of slippage.

1. Introduction

Wetting and dewetting of solids by liquids involve the movement over solid surfaces of the solid/liquid/gas (or liquid) line of contact, an understanding of whose motion is important in many circumstances. For example, to form good polymeric adhesive joints between solids (Schonhorn, Frisch & Kwei 1966), wetting of the solid by the melt before it solidifies is desired; to recover efficiently the crude oil from the pores of reservoir rocks by displacement with (immiscible) water (Taber 1969), a relation between the displacement rate and pressure is desired; when fibres and sheets are withdrawn from (or immersed into) liquids for surface treatment (Inverarity 1969), the maximum rate of withdrawal without the entrainment of bulk liquid is sought.

To understand the dynamics of the contact-line movement we must solve the Navier–Stokes equation for the flow of the liquid over the solid surface. The position of the moving liquid surface is not known *a priori* but must be determined to satisfy the equation and the boundary conditions. It may be found by assuming reasonable trial shapes of the liquid surface with a given dynamic contact angle‡ θ_d and then, after solving the Navier–Stokes equation, establishing which one satisfies the boundary conditions at the liquid surface. As pointed out by Huh & Scriven (1971), this approach to locating the position of the liquid surface fails because the normal stress on the liquid surface then varies inversely with distance from the contact line, so that it is impossible to satisfy the normal-stress boundary condition. This failure arises from a purely kinematic reason: for the contact line to move, adjacent liquid elements must

† Present address: Exxon Production Research Co., Houston, Texas 7701.

‡ Experimental values of the dynamic contact angle θ_d, the angle formed by the liquid interface and the solid surface at the moving contact line, are available in the literature (e.g. Elliott & Riddiford 1967) as a function of the contact-line velocity U for a number of spreading systems; however, efforts to predict θ_d theoretically as a function of U, the static contact angle θ_s and the properties of the liquid and solid have been generally unsuccessful.

be brought to (or removed from) the solid surface. Of necessity, the adjacent elements assume the velocity of the contact line, but at the same time they should not move on the solid surface if we enforce the conventional no-slip condition of fluid mechanics; doing this, however, creates a discontinuity in velocity at the contact line (Dussan V. & Davis 1974).

To resolve this anomaly various remedies are possible.

(i) The measured dynamic contact angles were obtained at low optical resolution and therefore could differ appreciably from the microscopic values if there is a severe meniscus deformation near the contact line due to flow. There is thus the possibility that the dynamic contact angle at the microscopic level is 180°; the liquid element would then roll onto (or peel from) the solid.

(ii) Near the contact line, there may exist a very small region where the continuum hydrodynamic equations are inadequate; the contact-line movement may be not a mechanical process but a surface diffusive process.

(iii) We may relax the no-slip condition at the solid/liquid interface.

Experimental observations of contact-line movement, which are being made in our laboratory and will be reported later, reveal that the rolling scheme with a dynamic contact angle of 180° cannot be a universal spreading mechanism. For example, dynamic contact angles of about 30° were observed in the scanning electron microscope at a resolution of about 1 μm when silicone oils spread on aluminium-coated smooth mica surfaces (Oliver, Huh & Mason 1977). The second possibility described above has been discussed by Hansen & Toong (1971*b*), who concluded that in the region of the contact line the classical concepts of fluid mechanics fail. However, they could not specify either the exact size of the region or how the fluid behaviour there is related to that in the continuum zone. In this paper, we explore the possibility of slippage.

The hypothesis that liquid immediately next to a solid does not slip relative to the solid has proved acceptable as a basic principle in fluid mechanics, but it should be remembered that it was deduced entirely from experiments. Many experiments have been performed to detect the slippage but have yielded inconclusive results (e.g. Bulkley 1931); exceptions, however, have been claimed when the liquid flows in a very narrow capillary tube with a resultant high wall stress (Derjaguin & Fedyakin 1969), and when certain polymers (Pearson 1966, p. 20) and non-wetting liquids (Tolstoi 1952*b*) presumably take a long time to adhere to the solid. For contact-line movement, the shear stress on the solid surface may be very large near the contact line as suggested by Huh & Scriven (1971); and as the liquid element is brought to the solid surface at the contact line, there will be a relaxation time during which the bonding of liquid molecules to the solid is incomplete. Therefore, while slippage is generally insignificant at liquid/solid interfaces, there is a distinct possibility that it is meaningful near the moving contact line during spreading.

To study this possibility, we consider the steady movement of a liquid meniscus displacing air or its own vapour in a circular capillary. The tube radius a is sufficiently small that the effect of gravity is negligible, i.e. $\rho g a^2/\gamma_L \ll 1$, where ρ is the liquid density, g is the acceleration due to gravity and γ_L is the surface tension of the liquid. We restrict our study to the systems for which the meniscus profile $z = h(r)$ in cylindrical co-ordinates r and z (see figure 1) is approximately flat everywhere, i.e.

$$|dh/dr| \ll 1, \quad \text{or} \quad \lambda \equiv |h_0/a| \ll 1,$$

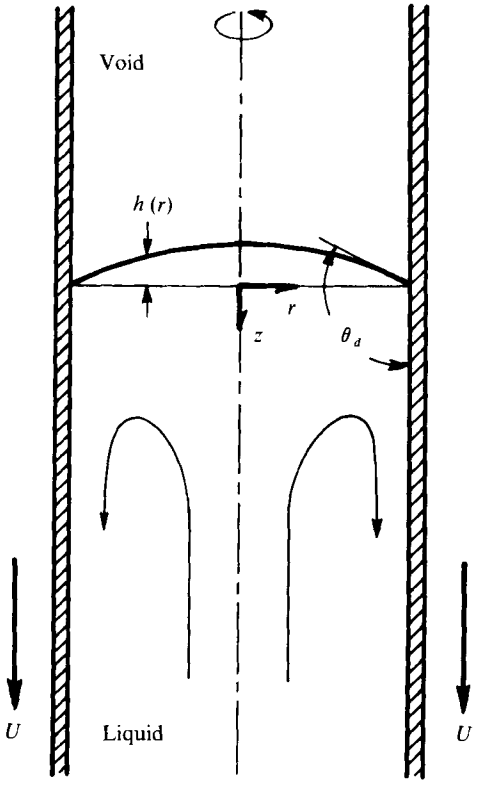

FIGURE 1. Schematic diagram of a liquid meniscus moving steadily in a circular capillary tube.

where h_0 is the meniscus height at $r = 0$ when $h = 0$ at $r = a$. By initially approximating $h \equiv 0$ and thus pre-empting the normal-stress condition at the liquid surface, Bhattacharji & Savic (1965) obtained the solution for the flow field accompanying the meniscus movement with no slippage of liquid on the solid. When we apply the normal-stress condition at the liquid surface ($z = 0$) to estimate $h(r)$, we fail because the initial assumption $|dh/dr| \ll 1$ cannot be observed near the contact line (see following section). To remedy the situation, we first replace the no-slip condition with the classical slippage boundary condition (Dryden, Murnaghan & Bateman 1956) that the slip velocity Δv is proportional to the shear stress T_s exerted on the solid (model I in figure 2):

$$T_s = \beta \Delta v \quad \text{for} \quad z \geqslant 0, \tag{1}$$

where β is the slip coefficient, so that $\beta = \infty$ represents the conventional no-slip condition. The characteristic length $l \equiv 2\mu/\beta$, where μ is the liquid viscosity, provides an indication of the size of the region near the contact line where slip is important.

We also consider a simple alternative slippage model. When an element of the spreading liquid is brought from the liquid/gas interface to the solid surface at $z = 0$, $r = a$, its direction of flow is suddenly changed and it is subjected to molecular interactions with the solid surface. The molecules of the liquid element which had been aligned at the liquid surface may then become disoriented; for them to be reoriented at the liquid/solid interface, a reorientation time τ is required (Hansen & Miotto 1957). In the region of width $l = U\tau$ from the contact line at the liquid/solid

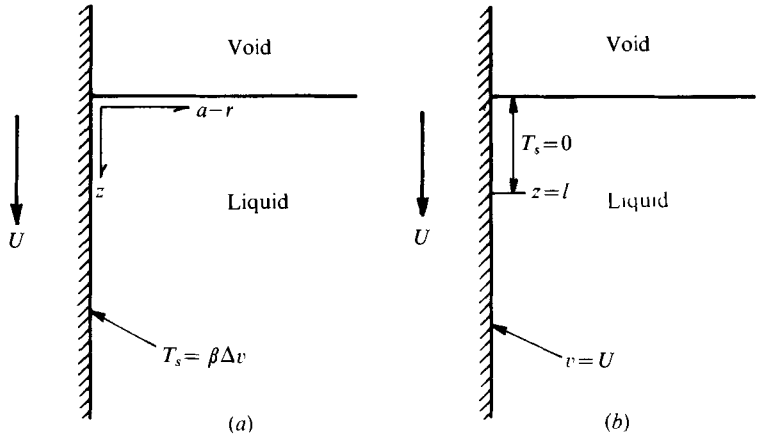

FIGURE 2. Hydrodynamic models of slippage. (*a*) Model I: classical slippage. (*b*) Model II: local slippage.

interface, where U is the contact-line velocity, re-orientation and bonding of the liquid molecules to the solid will occur, accompanied by slip of liquid on the solid. For this model (model II in figure 2), we assume that over the distance l the liquid slips freely, but thereafter the liquid/solid bonding has been completed and the no-slip boundary condition is observed on the solid surface:

$$T_s = 0 \quad \text{for} \quad 0 \leqslant z \leqslant l; \quad \Delta v = 0 \quad \text{for} \quad z > l. \tag{2}$$

In the next section, we consider model I and examine whether the difficulties encountered with the no-slip solution are removed. Since the exact solution of the Bhattacharji–Savic problem with the slippage boundary condition is difficult to obtain, we attempt an asymptotic solution, for $\epsilon \equiv l/a \ll 1$, which is valid uniformly over the entire flow region. This is done by obtaining a solution (by an outer expansion) which is valid away from the contact line but breaks down near it and another solution (by an inner expansion) which is valid near the contact line but breaks down away from it, and then matching the two solutions (Cole 1968). This matching technique has the advantage that, while the spreading problem can still be tackled with the no-slip condition for its appropriate flow domain except for the contact-line region, the anomaly in the contact-line region can be remedied locally. The flow behaviour near the contact line is examined, and the interfacial velocities, wall stress, pressure and meniscus shape are calculated. Model II is similarly studied in §3. In the last section, a modified version of the Washburn (1921) equation is given which takes account of the meniscus, and the significance of the experimental measurements of the dynamic contact angle is discussed.

2. Slippage Model I

To express the hydrodynamic problem of the meniscus movement in the simplest mathematical form, we employ the following dimensionless variables:

$$\xi \equiv r/a, \quad \eta \equiv z/a, \quad \phi \equiv \Phi/a^2U, \quad H \equiv h/\lambda a,$$

where Φ is the stream function defined by the two velocity components in the r and z directions respectively, i.e.

$$u \equiv r^{-1}\partial\Phi/\partial z, \quad v \equiv -r^{-1}\partial\Phi/\partial r. \tag{3}$$

If the Reynolds number $\rho a U/\mu$ is small, the flow field behind the meniscus formed by an incompressible Newtonian liquid can be determined by solving the creeping-flow approximation to the Navier–Stokes equation

$$\left(\frac{\partial^2}{\partial\xi^2}-\frac{1}{\xi}\frac{\partial}{\partial\xi}+\frac{\partial^2}{\partial\eta^2}\right)^2\phi = 0. \tag{4}$$

The boundary conditions to be applied are as follows.

(i) Vanishing normal component of velocity at the solid surface:

$$\phi = 0 \quad \text{at} \quad \xi = 1. \tag{5}$$

(ii) The slippage boundary condition, which from (1) is

$$\frac{\epsilon}{2}\frac{1}{\xi}\left(\frac{\partial^2\phi}{\partial\xi^2}-\frac{1}{\xi}\frac{\partial\phi}{\partial\xi}\right)+\frac{1}{\xi}\frac{\partial\phi}{\partial\xi} = -1 \quad \text{at} \quad \xi = 1, \tag{6}$$

where $\epsilon \equiv l/a \ll 1$.

(iii) Vanishing normal component of velocity at the liquid surface:

$$\lambda\frac{dH}{d\xi}\frac{\partial\phi}{\partial\eta}+\frac{\partial\phi}{\partial\xi} = 0 \quad \text{at} \quad \eta = \lambda H. \tag{7}$$

(iv) Vanishing tangential stress at the liquid surface:

$$2\lambda\frac{dH}{d\xi}\left(2\frac{\partial^2\phi}{\partial\xi\partial\eta}-\frac{1}{\xi}\frac{\partial\phi}{\partial\eta}\right)+\left\{1-\lambda^2\left(\frac{dH}{d\xi}\right)^2\right\}\left(\frac{\partial^2\phi}{\partial\xi^2}-\frac{1}{\xi}\frac{\partial\phi}{\partial\xi}-\frac{\partial^2\phi}{\partial\eta^2}\right) = 0 \quad \text{at} \quad \eta = \lambda H. \tag{8}$$

(v) The normal-stress condition at the liquid surface:

$$p+\frac{2}{\xi\{1+\lambda^2(dH/d\xi)^2\}}\left[\left\{1-\lambda^2\left(\frac{dH}{d\xi}\right)^2\right\}\frac{\partial^2\phi}{\partial\xi\partial\eta}+\frac{\lambda^2}{\xi}\left(\frac{dH}{d\xi}\right)^2\frac{\partial\phi}{\partial\eta}\right.$$
$$\left.-\lambda\frac{dH}{d\xi}\left(\frac{\partial^2\phi}{\partial\xi^2}-\frac{1}{\xi}\frac{\partial\phi}{\partial\xi}-\frac{\partial^2\phi}{\partial\eta^2}\right)\right] = \frac{\lambda}{\sigma}\left[\frac{d^2H/d\xi^2}{\{1+\lambda^2(dH/d\xi)^2\}^{\frac{3}{2}}}+\frac{\xi^{-1}dH/d\xi}{\{1+\lambda^2(dH/d\xi)^2\}^{\frac{1}{2}}}\right]$$
$$\text{at} \quad \eta = \lambda H, \tag{9}$$

where $\sigma \equiv \mu U/\gamma_L \ll 1$, $p \equiv aP/\mu U$ and P is the liquid pressure above that of the air.

The boundary conditions which should apply for the meniscus shape are

(vi) $$dH/d\xi = \lambda^{-1}\tan(\theta_d - 90°) \quad \text{at} \quad \xi = 1, \tag{10}$$

(vii) $$dH/d\xi = 0 \quad \text{at} \quad \xi = 0, \tag{11}$$

where $|\theta_d - 90°| \ll 1$, which, together with $\sigma \ll 1$, is generally required to maintain $\lambda \ll 1$ as we shall see later.

When $\sigma = 0$, (9) becomes the Young–Laplace equation defining the static meniscus profile, and $\theta_d \to \theta_e$; thus $p = (2/\sigma)\sin(\theta_e - 90°)$ or $P = (2\gamma_L/a)\sin(\theta_e - 90)°$ when there is no flow.

Because the position $\eta = \lambda H$ of the liquid surface is as yet unknown, we attempt a solution in the form of a power series in λ for the domain perturbation in the neighbourhood of $\eta = 0$:

$$\phi = \phi^{(0)} + \lambda\phi^{(1)} + \ldots, \tag{12}$$

where $\lambda \ll 1$. If the $\phi^{(i)}$ are analytic in η at $\eta = 0$, the boundary conditions at the liquid surface may be applied at $\eta = 0$, by expanding $\phi(\xi, \eta)$ in a Taylor series at $\eta = 0$:

$$\phi(\xi, \lambda H) = \phi^{(0)}(\xi, 0) + \lambda[\phi^{(1)}(\xi, 0) + H\partial\phi^{(0)}(\xi, 0)/\partial\eta] + \ldots. \tag{13}$$

Even though the successive terms of (12) can in principle be obtained by solving (4)–(9) by inserting (12) and (13), we restrict our consideration to the first term $\phi^{(0)}$. The boundary conditions (7)–(9) then become, respectively,

$$\phi^{(0)} = 0, \quad \partial^2\phi^{(0)}/\partial\eta^2 = 0 \quad \text{at} \quad \eta = 0, \tag{14), (15}$$

$$p^{(0)} + \frac{2}{\xi}\frac{\partial^2\phi^{(0)}}{\partial\xi\,\partial\eta} = \frac{\lambda}{\sigma}\left(\frac{d^2H}{d\xi^2} + \frac{1}{\xi}\frac{dH}{d\xi}\right) \quad \text{at} \quad \eta = 0, \tag{16}$$

where $p^{(0)}$ is the first term in the series expansion of p in λ. Equation (4) and the boundary conditions (5) and (6) will remain unchanged but with $\phi^{(0)}$ in place of ϕ. The stream function $\phi^{(0)}$ may now be obtained by solving (4) with the boundary conditions (5), (6), (14) and (15); the normal-stress condition (16) and the boundary conditions (10) and (11) then define the first estimate of the meniscus shape $\lambda H(\xi)$.

Since $\epsilon \ll 1$, we propose to solve for $\phi^{(0)}$ by employing the asymptotic matching technique (Cole 1968). However, no comprehensive treatment of the asymptotic expansions is attempted; we shall be content with application of the method to obtain the first-order matched solution, even though the higher-order terms can in principle be obtained.

An outer expansion

If we consider only the first term of the expansion of $\phi^{(0)}$ in ϵ, i.e.

$$\phi^{(0)} \sim \phi_0^{(0)}(\xi, \eta) + O(\epsilon), \tag{17}$$

the problem to be solved for $\phi_0^{(0)}$ is, from (4)–(6) and (14) and (15),

$$\left(\frac{\partial^2}{\partial\xi^2} - \frac{1}{\xi}\frac{\partial}{\partial\xi} + \frac{\partial^2}{\partial\eta^2}\right)^2 \phi_0^{(0)} = 0, \tag{18}$$

$$\phi_0^{(0)} = 0 \quad \text{at} \quad \xi = 1, \quad \eta = 0, \tag{19), (20}$$

$$\xi^{-1}\partial\phi_0^{(0)}/\partial\xi = -1 \quad \text{at} \quad \xi = 1, \tag{21}$$

$$\partial^2\phi_0^{(0)}/\partial\eta^2 = 0 \quad \text{at} \quad \eta = 0. \tag{22}$$

This is exactly the no-slip problem defined by Bhattacharji & Savic (1965), who obtained as its solution

$$\phi_0^{(0)} = \int_0^\infty C(k)\,\xi[I_0(k)\,I_1(k\xi) - \xi I_1(k)\,I_0(k\xi)]\frac{\sin k\eta}{k^2}\,dk, \tag{23}$$

where

$$C(k) \equiv 2/\pi[I_1^2(k) - I_0(k)\,I_2(k)]$$

and I_n is a modified Bessel function of order n. Even though Bhattacharji & Savic (1965) discussed in detail the flow field described by (23), they did not recognize that it resulted in an infinite force at $\xi = 1, \eta = 0$, as mentioned in the introduction. To show that $\phi_0^{(0)}$ is not a valid approximation for $\phi^{(0)}$ near the contact line, we make the change of variables

$$x \equiv (1-\xi)/\epsilon, \quad y \equiv \eta/\epsilon, \tag{24}$$

and express (23) in terms of these 'inner' variables:

$$\begin{aligned}\phi_0^{(0)} &= \epsilon \int_0^\infty C\left(\frac{\kappa}{\epsilon}\right)(1-\epsilon x)\left\{I_0\left(\frac{\kappa}{\epsilon}\right) I_1\left(\frac{\kappa}{\epsilon}-\kappa x\right) - (1-\epsilon x) I_1\left(\frac{\kappa}{\epsilon}\right) I_0\left(\frac{\kappa}{\epsilon}-\kappa x\right)\right\} \frac{\sin \kappa y}{\kappa^2}\, d\kappa \\ &= 2\pi^{-1}\epsilon \int_0^\infty x\, e^{-\kappa x} \frac{\sin \kappa y}{\kappa}\, d\kappa + O(\epsilon^2) \\ &= 2\pi^{-1}\epsilon x \tan^{-1}(y/x) + O(\epsilon^2). \end{aligned} \tag{25}$$

Here $k \equiv \kappa/\epsilon$ and we have used the expansion

$$I_n(z) \sim \frac{e^z}{(2\pi z)^{\frac{1}{2}}}\left(1 - \frac{4n^2-1}{8z} + \ldots\right).$$

The first term on the right-hand side of (25) approximates $\phi_0^{(0)}$ for the immediate neighbourhood of the contact line. This approximation is in fact a special case ($\phi = 90°$, $\mu_A = 0$ in their notation) of the no-slip solution obtained by Huh & Scriven (1971), who discussed in detail its inadequacy near the contact line. In particular, the normal stress at the approximate location $\eta = 0$ of the liquid surface according to this solution is

$$p^{(0)} + \frac{2}{\xi}\frac{\partial^2 \phi^{(0)}}{\partial \xi\, \partial \eta} \sim -\frac{4}{\pi(1-\xi)} \quad \text{as} \quad \xi \to 1. \tag{26}$$

Inserting this into (16), we see that the contact-angle condition (10) cannot be satisfied. It is therefore necessary to consider also a limit of $\phi^{(0)}$ as $\epsilon \to 0$ which retains information on the effect of slip near the contact line.

An inner expansion

To obtain an approximation to $\phi^{(0)}$ in the neighbourhood of the contact line, we expand $\phi^{(0)}$ in powers of ϵ in terms of the inner variables x and y as

$$\psi^{(0)} \equiv \phi^{(0)}/\epsilon \sim \psi_0^{(0)}(x, y) + O(\epsilon), \tag{27}$$

again restricting consideration to the first term of the expansion.

Equations (4)–(6) and (14) and (15) then become

$$\left(\frac{\partial^2}{\partial x^2} + \frac{\partial^2}{\partial y^2}\right)^2 \psi_0^{(0)} = 0, \tag{28}$$

$$\psi_0^{(0)} = 0 \quad \text{at} \quad x = 0, \quad y = 0, \tag{29), (30}$$

$$\partial^2 \psi_0^{(0)}/\partial y^2 = 0 \quad \text{at} \quad y = 0, \tag{31}$$

$$\frac{1}{2}\frac{\partial^2 \psi_0^{(0)}}{\partial x^2} - \frac{\partial \psi_0^{(0)}}{\partial x} = -1 \quad \text{at} \quad x = 0. \tag{32}$$

Employing the Fourier sine transform, we can derive the following integral as the formal solution of the problem thus defined:

$$\psi_0^{(0)} = \frac{2}{\pi}\int_0^\infty \frac{x e^{-kx}}{k(k+1)} \sin ky\, dk, \tag{33}$$

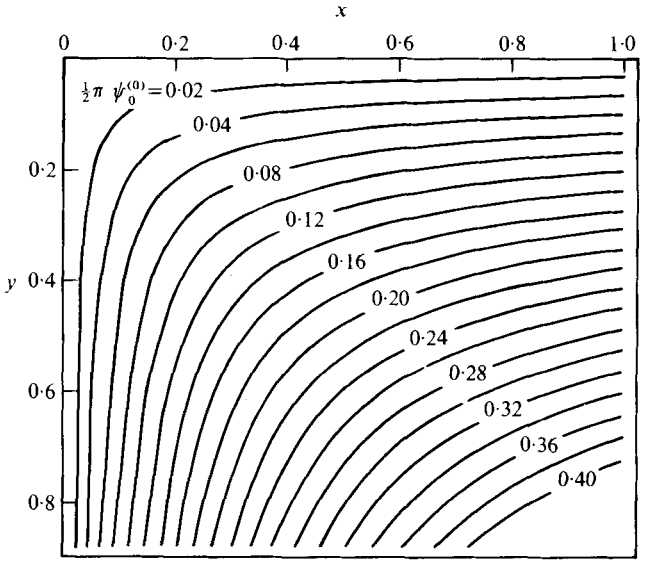

FIGURE 3. Streamlines near the contact line for model I. $x \equiv (a-r)/l$ and $y \equiv z/l$.

which can be expressed in an infinite series as

$$\psi_0^{(0)} = \frac{2}{\pi} x[\omega + \mathrm{Im}\{e^{x+iy}E_1(x+iy)\}]$$

$$= \frac{2}{\pi} x\left[\omega - e^x\left\{\omega\cos y + (\gamma + \ln\zeta)\sin y + \sum_{n=1}^{\infty}\frac{(-1)^n\zeta^n}{nn!}\sin(n\omega+y)\right\}\right], \qquad (34)$$

where $\zeta \equiv (x^2+y^2)^{\frac{1}{2}}$, $\omega \equiv \tan^{-1}(y/x)$, E_1 is the exponential integral, $\gamma = 0{\cdot}5772\ldots$ is the Euler constant, and Im { } designates the imaginary part of the argument. The infinite series in (34) converges rapidly and figure 3 shows the streamlines at the corner, calculated by taking the first ten terms of the series in (34). The flow velocity is single-valued ($= 0$) at the contact line ($\zeta = 0$). Very near the contact line, the shear stress component attains a finite value

$$-\frac{a}{U}\left(\frac{\partial u}{\partial z}+\frac{\partial v}{\partial r}\right) \sim \frac{1}{\epsilon}\left(\frac{\partial^2\psi_0^{(0)}}{\partial x^2}-\frac{\partial^2\psi_0^{(0)}}{\partial y^2}\right) \sim \frac{4}{\pi\epsilon}(\omega-\sin 2\omega)+O(\zeta),$$

but the normal stress components and the pressure p still show a weak singularity at $\zeta = 0$:

$$-\frac{2a}{U}\frac{\partial v}{\partial z}\left[\text{or}\quad \frac{2a}{U}\frac{\partial u}{\partial r}\quad \text{or}\quad P\Big/\left(\mu\frac{U}{a}\right)\right] \sim \frac{4}{\pi\epsilon}\ln\zeta + O(1).$$

It can also be deduced from (34) that at the contact line only a logarithmic singularity occurs in the viscous dissipation function, which becomes finite when integrated over a liquid volume including the contact line. The contact-line movement is therefore not accompanied by an infinite rate of viscous dissipation, as predicted by the no-slip solution. The flow field defined by (34) has thus proved to be free of the inadequacies discussed by Huh & Scriven (1971).

A matched solution

By matching the above two solutions, which are respectively valid away from and near the contact line, we can obtain a solution which is uniformly valid for the entire flow region. For this purpose, we express the outer expansion in terms of the inner variables as in (25); we also express the inner expansion in terms of the outer variables:

$$\psi_0^{(0)} = \frac{2}{\pi}\frac{(1-\xi)}{\epsilon}\int_0^\infty \frac{\exp[-\kappa(1-\xi)]}{\kappa(1+\epsilon\kappa)}\sin\kappa\eta\, d\kappa \tag{35a}$$

$$= \frac{2}{\pi}\frac{(1-\xi)}{\epsilon}\tan^{-1}\left(\frac{\eta}{1-\xi}\right) + O(1). \tag{35b}$$

A uniformly valid composite expansion can be obtained by adding (23) and (33) and subtracting the common part $(2/\pi)\epsilon x\tan^{-1}(y/x)$ (Cole 1968, p. 13):

$$\begin{aligned}\phi^{(0)} &\sim \phi_0^{(0)} + \epsilon\psi_0^{(0)} - 2\pi^{-1}\epsilon x\tan^{-1}(y/x)\\ &= \int_0^\infty C(k)\,\xi[I_0(k)I_1(k\xi) - \xi I_1(k)I_0(k\xi)]\frac{\sin k\eta}{k^2}\,dk\\ &\quad + \frac{2}{\pi}\epsilon x\left[\int_0^\infty \frac{e^{-kx}\sin ky}{k(k+1)}\,dk - \tan^{-1}\left(\frac{y}{x}\right)\right].\end{aligned} \tag{36}$$

The velocity on the meniscus can be likewise calculated as

$$\begin{aligned}\frac{u(r,0)}{U} &\sim \frac{1}{\xi}\frac{\partial\phi_0^{(0)}}{\partial\eta}(\xi,0) + \frac{\partial\psi_0^{(0)}}{\partial y}(x,0) - \frac{2}{\pi}\\ &= \int_0^\infty C(k)\,[I_0(k)I_1(k\xi) - \xi I_1(k)I_0(k\xi)]\frac{dk}{k} + \frac{2}{\pi}(x\,e^x E_1(x) - 1).\end{aligned} \tag{37}$$

Figure 4 shows $u(r,0)/U$ as a function of ξ for various values of ϵ. The integral in (37), and the other integrals which follow, was calculated numerically using the Gaussian–Laguerre quadrature formula with 16 divisions. We see that with the outer expansion alone $u(r\to a,0) = 2U/\pi$; with the addition of the inner expansion, the velocity sharply decreases near the contact line and becomes zero at the line. The liquid velocity on the solid surface is

$$\begin{aligned}\frac{v(a,z)}{U} &\sim -\frac{1}{\xi}\frac{\partial\phi_0^{(0)}}{\partial\xi}(1,\eta) + \frac{\partial\psi_0^{(0)}}{\partial x}(0,y) - 1\\ &= 1 - 2\pi^{-1}[\mathrm{ci}\,y\sin y - \mathrm{si}\,y\cos y]\end{aligned} \tag{38}$$

where ci and si are the cosine and sine integrals, respectively (Abramowitz & Stegun 1965, p. 231). At the contact line, the velocity is zero, but $v(a,z) = U$ is rapidly attained away from the line. The shear stress T_s on the solid wall becomes

$$\begin{aligned}\frac{T_s}{\mu U/a} &\sim \frac{1}{\xi}\left(\frac{\partial^2\phi_0^{(0)}}{\partial\xi^2} - \frac{1}{\xi}\frac{\partial\phi_0^{(0)}}{\partial\xi}\right)(1,\eta) + \frac{1}{\epsilon}\frac{\partial^2\psi_0^{(0)}}{\partial x^2}(0,y) + \frac{4}{\pi\eta}\\ &= -2\int_0^\infty C(k)\,I_1^2(k)\frac{\sin k\eta}{k}\,dk - \frac{4}{\pi\epsilon}\left[\mathrm{ci}\,y\sin y - \mathrm{si}\,y\cos y - \frac{1}{y}\right].\end{aligned} \tag{39}$$

Figure 5 shows $T_s/(\mu U/a)$ as a function of η for various ϵ. With the no-slip condition, $T_s \sim -4\mu U/\pi z$ near the contact line; with slip, the stress becomes bounded at the

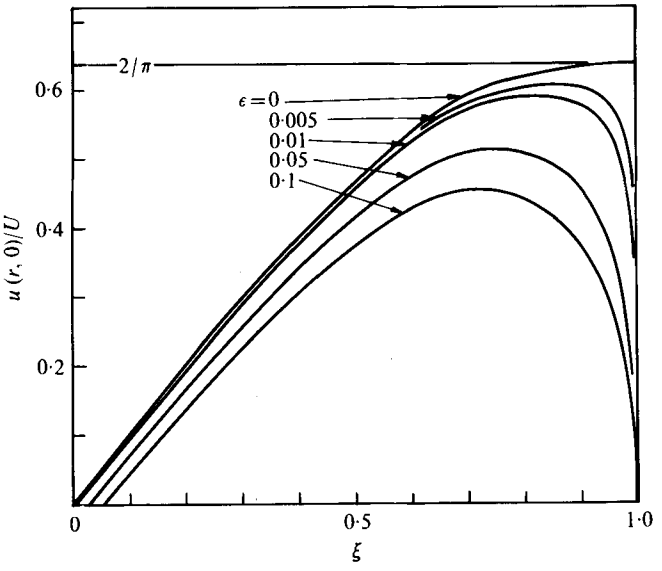

FIGURE 4. Liquid velocity on the meniscus ($z = 0$).

contact line, where $T_s = -2\mu U/l = U/\beta$, which is equivalent to the wall stress for Poiseuille flow in a tube of radius $2l$. When z is large, $T_s \to -4\mu U/a$, the value for Poiseuille flow in the tube of radius a being considered.

The normal stress T_n on the meniscus ($z = 0$) can be calculated as

$$\frac{T_n}{\mu U/a} \sim p^{(0)} + \frac{2}{\xi}\frac{\partial^2 \phi^{(0)}}{\partial \xi\, \partial \eta}$$
$$= 2\int_0^\infty C(k)\left[\{kI_0(k) - 2I_1(k)\}I_0(k\xi) - k\xi I_1(k)I_1(k\xi) - I_1(k)\{I_0(k\xi) - 1\}\right]\frac{dk}{k}$$
$$+ \frac{4}{\pi\epsilon}\left[1 - e^x E_1(x)(2+x) + \frac{1}{x}\right] + p_A, \tag{40}$$

where $P_A \equiv \mu U p_A/a$ is the liquid pressure at the apex ($r = z = 0$) of the meniscus with respect to the constant air pressure. Figure 6 shows $T_n'/(\mu U/a)$ as a function of ξ, where

$$T_n' \equiv T_n - \mu\frac{U}{a}\left\{\int_0^\infty 2C(k)\left[kI_0(k) - 2I_1(k)\right]\frac{dk}{k} + p_A\right\}$$

and

$$\int_0^\infty C(k)\left[kI_0(k) - 2I_1(k)\right]\frac{dk}{k} = 2{\cdot}034.$$

We can see that, with the outer expansion alone, $T_n \sim -4\mu U/\pi(a-r)$ near the contact line; with the addition of the inner expansion, the singularity at the contact line still remains but $T_n \sim (8\mu U/\pi l)\ln(a-r)$.

The approximate meniscus profile $z = h(r)$ can be calculated by inserting (40) into (16). Integrating (16) with the boundary condition (11), we obtain

$$\frac{\lambda}{\sigma}\frac{dH}{d\xi} \sim 2\int_0^\infty C(k)\left[\{kI_0(k) - I_1(k)\}I_1(k\xi) + \tfrac{1}{2}k\xi I_1(k) - k\xi I_1(k)I_0(k\xi)\right]\frac{dk}{k^2}$$
$$+ 4\pi^{-1}\left[(x+1)e^x E_1(x) - 1\right] + \tfrac{1}{2}p_A\xi. \tag{41}$$

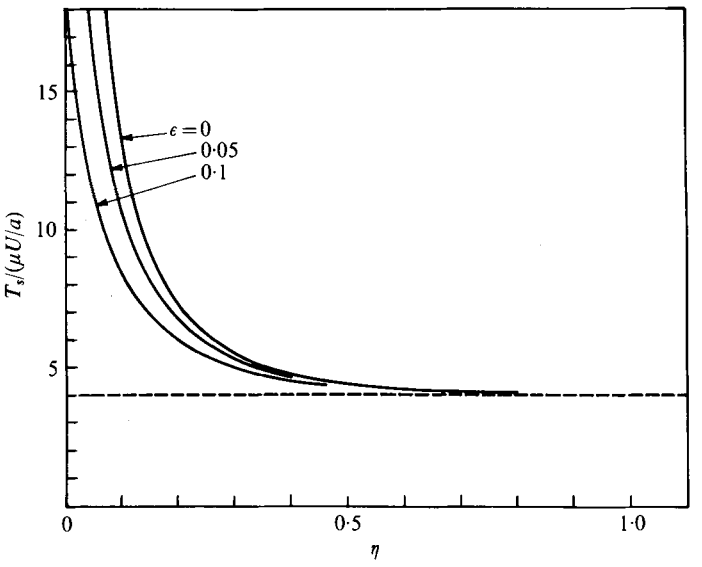

FIGURE 5. Shear stress exerted on the tube wall.

The integral term in (41) becomes $4\pi^{-1}\ln(1-\xi)+2{\cdot}53\ldots$ as $\xi\to 1$, where the numerical constant is obtained by the numerical integration of the integral. By applying the boundary condition (10) and matching the inner and outer expansions, we obtain

$$p_A = 2\sigma^{-1}[\tan(\theta_d - 90°) - 4\sigma\pi^{-1}(\ln\epsilon + 0{\cdot}410)]. \tag{42}$$

To show the meniscus deformation due to viscous forces, we plot in figure 7 the variation in meniscus slope expressed as

$$S \equiv \frac{1}{\sigma}\left[\lambda\frac{dH}{d\xi} - \xi\tan(\theta_d - 90°)\right] = \left[\frac{dh}{dr} - \frac{r}{a}\tan(\theta_d - 90°)\right]\Big/\left(\mu\frac{U}{\gamma_L}\right) \tag{43}$$

as a function of ξ. We see that, except in the neighbourhood of the contact line, the meniscus slope is almost linear, i.e. the meniscus has a spherical shape similar to a static one when $\epsilon \ll 1$. As $\epsilon\to 0$, the non-spherical region becomes condensed, with severe meniscus deformation near the contact line.

Equation (41) can be integrated once more for the meniscus profile

$$\begin{aligned}\frac{\lambda H}{\sigma} \sim \int_0^\infty C(k)\,[\{I_0(k)+I_2(k)\}\{I_0(k\xi)-I_0(k)\} + \tfrac{1}{2}kI_1(k)\,(\xi^2-1)\\ - 2I_1(k)\{\xi I_1(k\xi) - I_1(k)\}]\frac{dk}{k^2} - \frac{4}{\pi}\epsilon x e^x E_1(x) + \tfrac{1}{4}p_A(\xi^2-1),\end{aligned} \tag{44}$$

where we have applied the arbitrary boundary condition $H = 0$ at $\xi = 1$ ($x = 0$). At $\xi = 0$ ($x\to\infty$), $H = \pm 1$ by definition of λ (with the plus sign for $h_0 > 0$ and the minus sign for $h_0 < 0$), thus

$$\begin{aligned}\lambda &\sim \left|\sigma\int_0^\infty C(k)\,[\{I_0(k)+I_2(k)\}\{I_0(k)-1\} + I_1(k)\{\tfrac{1}{2}k - 2I_1(k)\}]\frac{dk}{k^2}\right.\\ &\qquad \left. + \tfrac{1}{2}\tan(\theta_d - 90°) - \tfrac{1}{2}\pi\sigma(\ln\epsilon + 0{\cdot}410)\right|\\ &= |\tfrac{1}{2}\tan(\theta_d - 90°) - \sigma(\tfrac{1}{2}\pi\ln\epsilon + 0{\cdot}429)|,\end{aligned} \tag{45}$$

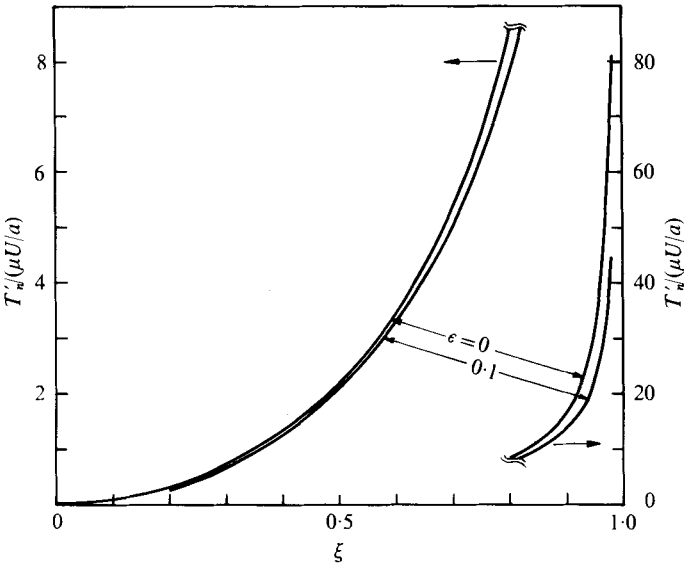

FIGURE 6. Normal stress on the meniscus ($z = 0$).

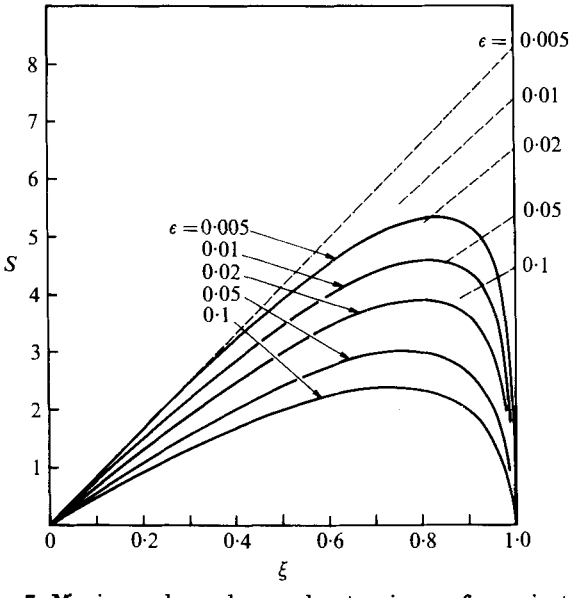

FIGURE 7. Meniscus slope change due to viscous forces in terms of

$$S \equiv \left[\lambda \frac{dH}{d\xi} - \xi \tan(\theta_d - 90°)\right] \Big/ \sigma = \left[\frac{dh}{dr} - \frac{r}{a}\tan(\theta_d - 90°)\right] \Big/ \left(\mu \frac{U}{\gamma_L}\right).$$

The dotted lines represent the slope change for the apparent spherical meniscus profile defined by (57).

which when $\sigma = 0$, for the static system, becomes $\lambda = \frac{1}{2}|\tan(\theta_e - 90°)|$. We see that for $\lambda \ll 1$ we need $\sigma \ll 1$ and $|\theta_a - 90°| \ll 1$ in general. These two restrictions are consistent with our other assumptions, since $\rho g a^2/\gamma_L \ll 1$ and $\epsilon \ll 1$ can be maintained independently of the above, and $\sigma \ll 1$ can easily yield $\rho a U/\mu \ll 1$. In the special case in which $\lambda = 0$ while $H \not\equiv 0$, another perturbation parameter which characterizes the departure of the meniscus shape from $\eta = 0$ should be employed instead of λ.

3. Slippage model II

For model II (figure 2*b*), (4)–(11) still apply, except that the slip boundary condition (6) is now replaced by

$$\left.\begin{aligned} \frac{\partial^2\phi}{\partial\xi^2} - \frac{1}{\xi}\frac{\partial\phi}{\partial\xi} = 0 \quad &\text{for} \quad 0 \leqslant \eta \leqslant \epsilon \\ \frac{1}{\xi}\frac{\partial\phi}{\partial\xi} = -1 \quad &\text{for} \quad \eta > \epsilon \end{aligned}\right\} \quad \text{at} \quad \xi = 1, \tag{46}$$

which is the non-dimensionalized form of (2). The first term $\phi_0^{(0)}$ of the outer expansion inserted into (46) again produces (21), so that the solution for $\phi_0^{(0)}$ is again (23) and identical to that for model I. For the inner expansion, (28)–(31) apply without modification, but instead of (32) we have

$$\left.\begin{aligned} \partial^2\psi_0^{(0)}/\partial x^2 = 0 \quad &\text{for} \quad 0 \leqslant y \leqslant 1 \\ \partial\psi_0^{(0)}/\partial x = 1 \quad &\text{for} \quad y > 1 \end{aligned}\right\} \quad \text{at} \quad x = 0. \tag{47}$$

Garabedian (1966) obtained the solution of the problem thus defined for $\psi_0^{(0)}$:

$$\psi_0^{(0)} = 2\pi^{-1}x\sin^{-1}\{\tfrac{1}{2}[x^2 + (y+1)^2]^{\frac{1}{2}} - \tfrac{1}{2}[x^2 + (y-1)^2]^{\frac{1}{2}}\}. \tag{48}$$

We can again demonstrate that various abnormalities encountered with the no-slip solution are resolved by permitting slip. Figure 8 shows the streamlines at the corner calculated from (48). We see that the flow velocity is again single-valued ($= 0$) at the contact line. Because the boundary condition on the solid surface changes from no tangential stress to no slip at $y = 1$, a weak singularity in the viscous stress tensor occurs there. Very near this point, the components of the stress tensor and the pressure p behave in accordance with

$$-\frac{a}{U}\left(\frac{\partial u}{\partial z} + \frac{\partial v}{\partial r}\right) \sim \frac{1}{\epsilon}\left(\frac{\partial^2\psi_0^{(0)}}{\partial x^2} - \frac{\partial^2\psi_0^{(0)}}{\partial y^2}\right) \sim \frac{1}{\pi\epsilon}\frac{\cos\omega'(1+\sin\omega'+2\sin^2\omega')}{[\zeta'(1+\sin\omega')]^{\frac{1}{2}}},$$

$$-2\frac{a}{U}\frac{\partial v}{\partial z}\left[\text{or} \quad 2\frac{a}{U}\frac{\partial u}{\partial r}\right] \sim -\frac{2}{\epsilon}\frac{\partial^2\psi_0^{(0)}}{\partial x\,\partial y} \sim -\frac{1}{2\pi\epsilon}\frac{(1+2\sin\omega'+\sin^2\omega')}{[\zeta'(1+\sin\omega')]^{\frac{1}{2}}},$$

$$P\Big/\left(\mu\frac{U}{a}\right) \sim -\frac{4}{\pi\epsilon}\frac{\cos(\frac{1}{4}\pi + \frac{1}{2}\omega')}{(2\zeta')^{\frac{1}{2}}}.$$

where $$\zeta' \equiv [x^2 + (y-1)^2]^{\frac{1}{2}}, \quad \omega' \equiv \tan^{-1}[(y-1)/x].$$

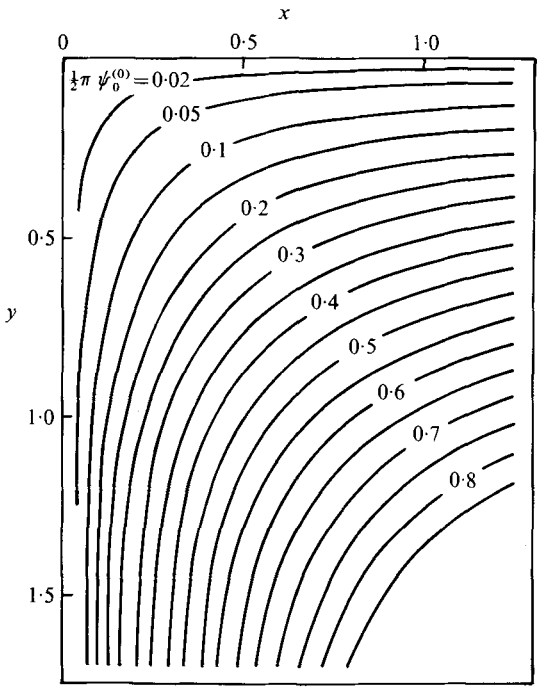

FIGURE 8. Streamlines near the contact line for model II. $x \equiv (a-r)/l$ and $y \equiv z/l$.

It can also be seen that no infinitely large amount of viscous dissipation occurs near the contact line. Therefore the flow field described by (48) is likewise free of the inadequacies discussed by Huh & Scriven (1971).

The inner and outer solutions can be matched in exactly the same manner as with model I. The inner expansion $\psi_0^{(0)}$ in terms of the outer variables again results in (35*b*). The inner-expansion terms for (37)–(39) are given by

$$\frac{\partial \psi_0^{(0)}}{\partial y}(x,0) = \frac{2}{\pi}\frac{x}{(1+x^2)^{\frac{1}{2}}}, \tag{49}$$

$$\frac{\partial \psi_0^{(0)}}{\partial x}(0,y) = \begin{cases} 2\pi^{-1}\sin^{-1}y & \text{for } 0 \leqslant y \leqslant 1, \\ 1 & \text{for } y > 1, \end{cases} \tag{50}$$

$$\frac{1}{\epsilon}\frac{\partial^2 \psi_0^{(0)}}{\partial x^2}(0,y) = \begin{cases} 0 & \text{for } 0 \leqslant y \leqslant 1, \\ -4/\pi\epsilon(y^2-1)^{\frac{1}{2}} & \text{for } y > 1. \end{cases} \tag{51}$$

Figures 9–11 compare these quantities for models I and II. Equation (51) shows that for model II the liquid freely slips from the contact line ($z = 0$) to the point $z = l$, and then near $z = l$ for $z > l$, the shear stress $T_s \sim -4\mu U/\pi[2l(z-l)]^{\frac{1}{2}}$, which becomes finite when integrated along the solid surface including the contact line.

The equations corresponding to (40)–(42) and (44) are

$$T_n \Big/ \left(\mu \frac{U}{a}\right) \sim \text{Int}\,(40) - \frac{4}{\pi\epsilon}\left[(1+x^2)^{-\frac{1}{2}} + (1+x^2)^{-\frac{3}{2}} - \frac{1}{x}\right] + p_A, \tag{52}$$

$$\frac{\lambda}{\sigma}\frac{dH}{\partial \xi} \sim \text{Int}\,(41) + \frac{4}{\pi}\left[\frac{x}{(1+x^2)^{\frac{1}{2}}} + \ln\{x + (1+x^2)^{\frac{1}{2}}\} - \ln 2x - 1\right] + \tfrac{1}{2}p_A\xi, \tag{53}$$

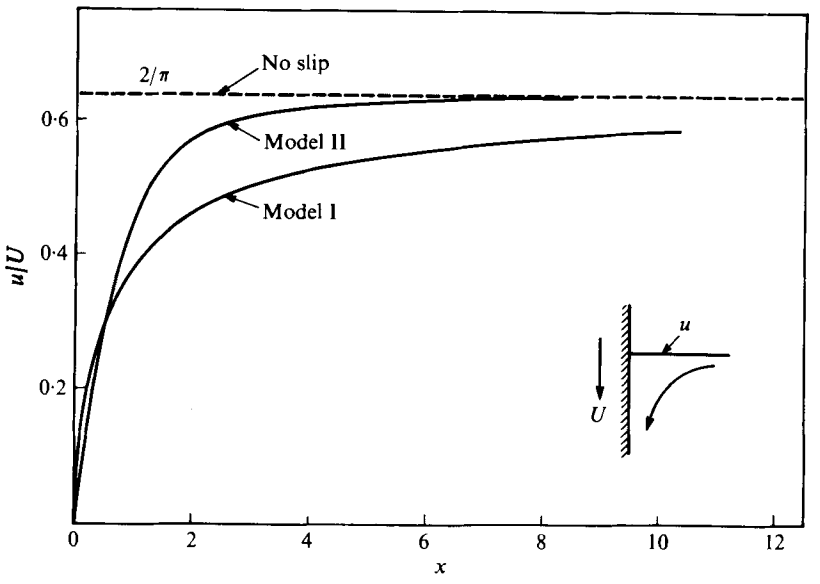

FIGURE 9. Liquid velocity on the meniscus near the contact line: comparison of the no-slip, model I and model II solutions.

$$p_A = 2\sigma^{-1}[\tan(\theta_d - 90°) - 4\sigma\pi^{-1}(\ln\epsilon + 0{\cdot}294)], \tag{54}$$

$$\frac{\lambda}{\sigma}H \sim \text{Int}\,(44) - \frac{4}{\pi}\epsilon\Big[(1+x^2)^{\frac{1}{2}} + \frac{1}{2}\Big(x + (1+x^2)^{\frac{1}{2}} - \frac{1}{x+(1+x^2)^{\frac{1}{2}}}\Big)\ln[x+(1+x^2)^{\frac{1}{2}}] - \frac{1}{2}\Big(x+(1+x^2)^{\frac{1}{2}} + \frac{1}{x+(1+x^2)^{\frac{1}{2}}}\Big) - x\ln 2x\Big] + \tfrac{1}{4}p_A(\xi^2-1), \tag{55}$$

where Int (i) designates the integral term in equation (i).

4. Discussion

To calculate the flow field and the meniscus profile from our equations, we must know l. For model I, an approximate theory was proposed by Tolstoi (1952*a*) to predict it:

$$l = 2d[\exp\{\alpha\pi d^2\gamma_L(1-\cos\theta_e)/kT\} - 1], \tag{56}$$

where d is the average diameter of a liquid molecule, k is the Boltzmann constant, T is the absolute temperature and α is a molecular parameter taken to be $\frac{1}{6}$ by Tolstoi. For mercury on glass at 20 °C, Tolstoi (1952*b*) deduced from his measurements that $l \simeq 0{\cdot}45$–$0{\cdot}49$ μm. When (56) was used for the same system with $\gamma_L = 490$ dyne/cm and $d = 0{\cdot}3$ nm, he obtained $l = 14{\cdot}4$ μm if $\theta_e = 140°$ and $l = 0{\cdot}18$ μm if $\theta_e = 90°$. Thus l is seen to be very sensitive to θ_e, with $l = 0$ when $\theta_e = 0$. For systems with small θ_e, indeed, the slip mechanism might not be realistic and the surface diffusive scheme may be more plausible.

For model II, there appears to be no appropriate theory to calculate the reorientation time $\tau \equiv l/U$ of the liquid molecules on the solid; this aspect of the problem

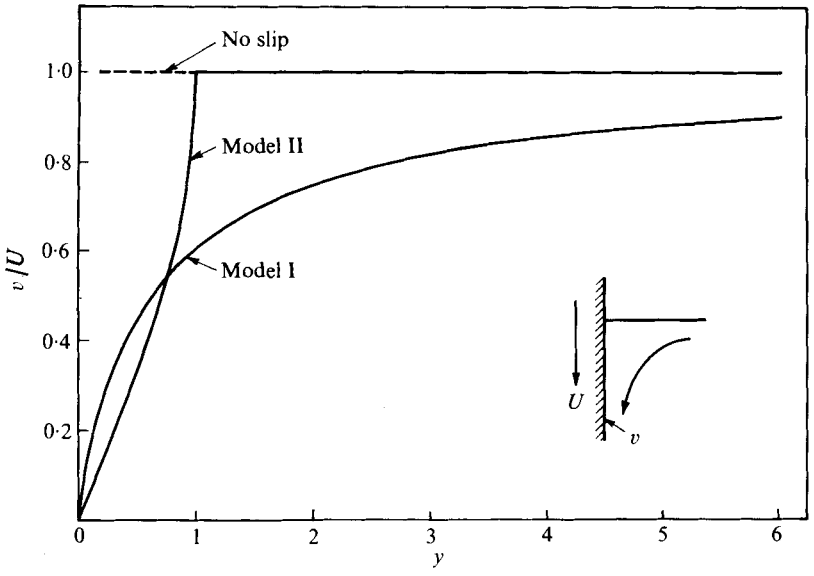

FIGURE 10. Liquid velocity on the solid surface near the contact line: comparison of the no-slip model I and model II solutions.

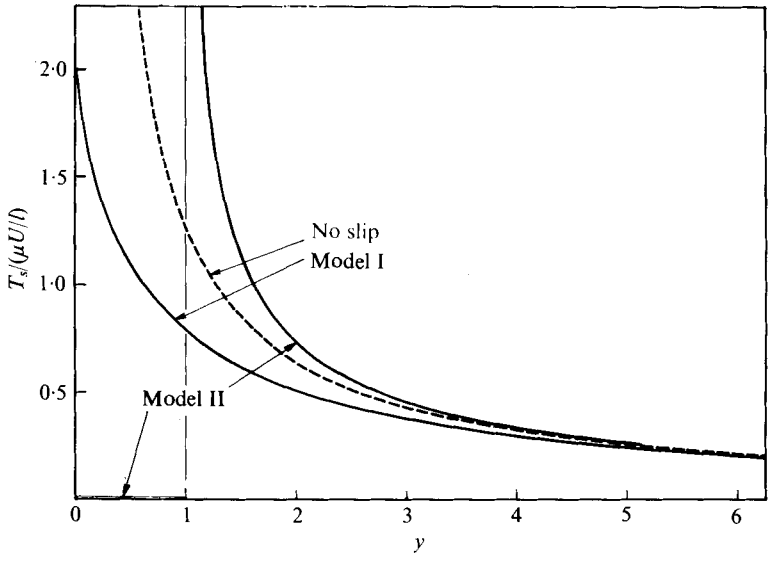

FIGURE 11. Shear stress on the solid surface near the contact line: comparison of the no-slip, model I and model II solutions.

warrants further study from the molecular, rather than continuum, point of view. The observations of Elliott & Riddiford (1967) pose an interesting possibility for model II: they reported that for very small U's the dynamic advancing contact angle was identical to the static angle, but that at a certain U_c the dynamic contact angle suddenly started to increase. We propose the possibility that the slip length l ($\equiv \tau U$) at U_c was identical to the dimension d of the liquid molecules; only when $U > U_c$, will l being

larger than d have any physical sense of slippage, which may have been revealed as the sudden increase in the dynamic contact angle. One crude approximation we might make is then $\tau \sim d/U_c$, and thus $l \simeq Ud/U_c$.

Whereas model I assumes that l is independent of U, it is proportional to U in model II. The above argument poses another possibility: that l does not represent true slippage but merely recognizes the fact that the liquid consists of molecules of finite size. Then our slippage scheme serves to remove the mathematical singularity inherent in the continuum formulation of the hydrodynamic problem with the no-slip boundary condition. The slip length is then again independent of U, and would be of the order of magnitude of d.

In many studies the dynamic contact angle $\theta_{\exp}$ was measured as a function of U, and attempts were made to correlate it with θ_e, μ, γ_L and other parameters. One unsettling question is whether or not the measured $\theta_{\exp}$ was indeed θ_d, with no instances of falsely identifying as θ_d the meniscus slope angle at a small distance from the actual contact line. If severe deformation of the meniscus occurs near the contact line owing to viscous forces, as Hansen & Toong (1971*b*) pointed out, the significance of the θ_d measurements will therefore be in doubt.

Using the approximate meniscus shape which we have calculated, we can estimate the viscous deformation of the meniscus near the contact line, to examine whether such measurements are erroneous. Because the severe meniscus deformation is concentrated near the contact line with $\epsilon \ll 1$, and the meniscus shape except for the contact-line region is almost the same as the static one (see figure 7), an apparent contact angle θ_{app} can be defined which would result in a static pressure equivalent to T_n at the meniscus apex. From (40), we obtain

$$p_A + 4{\cdot}068 = 2\sigma^{-1} \tan(\theta_{\text{app}} - 90°). \tag{57}$$

Combining this with (42) for model I, we get

$$\theta_{\text{app}} = \theta_d - 4\pi^{-1}\sigma(\ln\epsilon - 1{\cdot}188), \tag{58}$$

provided that θ_{app} and θ_d are close to 90°. The corresponding equation obtainable from (54) for model II is practically identical to (58), which may therefore be used for both models. The change $\theta_{\text{app}} - \theta_d$ in the meniscus slope angle thus serves as an estimate of the viscous deformation of the meniscus. The dashed lines in figure 7 show the slope change for the apparent spherical meniscus profiles when $\theta_d = 0$, i.e.

$$-4\pi^{-1}(\ln\epsilon - 1{\cdot}188)\xi.$$

To estimate $\theta_{\text{app}} - \theta_d$ for the systems which have been employed in the literature to measure dynamic contact angles, we must know l for the systems; because this is not available, we shall set l equal to a lower bound of 1 nm (10^{-7} cm), and thus obtain the largest possible deformation due to viscous forces. For the first two systems in table 1, which are taken from the data of Hoffman (1975), the viscous deformation could indeed be large, and it is almost certain that θ_d has not been measured. In table 1, we also list the experimentally measured values of $\theta_{\exp} - \theta_e$. The calculated $\theta_{\text{app}} - \theta_d$ for $l = 1$ nm is of the same order of magnitude as the experimental values of $\theta_{\exp} - \theta_e$ of Hoffmann (1975), thus suggesting the possibility that θ_d was in fact θ_e and that $\theta_{\exp}$, which he measured as the dynamic contact angle, was θ_{app}. Hoffman himself implied this by using the term 'apparent' contact angle. Because we assumed $l = 1$ nm, which should be of comparable magnitude with the diameter of the liquid molecules, we might

System	$U \times 10^3$ (cm/s)	$(\mu U/\gamma_L) \times 10^2$	Calculated $\theta_{app} - \theta_d$	$\theta_{exp} - \theta_e$ (experimental)
Admex 760/air/glass	0.847	2.11	23·1°	21°
$\theta_e = 69°$, $a = 0{\cdot}978$ mm	1·98	4·94	54·0°	45°
(Hoffman 1975)	2·07	5·16	56·4°	42°
	2·96	7·38	80·7°	45°
	3·02	7·53	82·3°	47°
Santicizer 405/air/glass	1·86	0·48	5·2°	1·7°
$\theta_e = 67°$, $a = 0{\cdot}978$ mm	3·46	0·89	9·7°	8·2°
(Hoffman 1975)	5·26	1·36	14·9°	17·6°
	16·9	4·36	47·7°	48°
	26·3	6·79	74·2°	54°
Nujol/air/glass	10·9	0·0635	0·7°	4°
$\theta_e = 21°$, $a = 1{\cdot}19$ mm	22·7	0·132	1·5°	10°
(Hansen & Toong 1971*a*)	33·7	0·196	2·2°	13°
	56·7	0·330	3·7°	18°
	73·4	0·428	4·7°	20°
Nujol/air/glass	40	0·140	1·4°	11°
$\theta_e = 23°$, $a = 0{\cdot}33$ mm	80	0·279	2·8°	20°
(Rose & Heins 1962)	120	0·419	4·2°	27°
	160	0·558	5·7°	34°
	200	0·698	7·1°	42°

TABLE 1. Meniscus deformation due to viscous forces, in terms of $\theta_{app} - \theta_d$ [see (58)]. $l = 1$ nm is used as a lower bound for the slip length.

further suggest that employing the slip condition but assuming $l \simeq d$ is necessary merely to remove the mathematical singularity arising from the continuum formulation of the hydrodynamic problem with the no-slip condition.

For the last two systems in table 1, which are taken from the experimental data of Hansen & Toong (1971*a*) and Rose & Heins (1962), the viscous deformation is relatively small, even though the application of (58) for such systems with low values of θ_{exp} would strictly be inappropriate. Here it appears that θ_d is truly different from θ_e and varies with U. A theoretical study by Miller & Ruckenstein (1974) supports this point, showing that the deviation of the contact angle from θ_e causes either wetting (advancement of the contact line) or dewetting (recession).

When a liquid slowly penetrates into a circular capillary tube, the Washburn (1921) equation describes approximately the relation between the displacement pressure P and the meniscus speed U:

$$U = (P + 2\gamma_L a^{-1} \cos\theta_d)\, a^2/8\mu L, \tag{59}$$

where L is the length of the liquid penetration. In deriving this equation, the viscous stress is given by that for conventional Poiseuille flow, which takes no account of the presence of the meniscus. From our derivation, we can calculate the liquid pressure at $z = L$, $r = 0$:

$$P \sim 2\mu \frac{U}{a} \int_0^\infty C(k) \left[\{kI_0(k) - 2I_1(k)\} \cos\left(k\frac{L}{a}\right) - I_1(k) \left\{ \cos\left(k\frac{L}{a}\right) - 1 \right\} \right] \frac{dk}{k} + \frac{2\gamma_L}{a} \tan(\theta_d - 90°) - \frac{8}{\pi} (\ln\epsilon + 0{\cdot}410) \left(\mu \frac{U}{a}\right), \tag{60}$$

in which for P_A we have used (42), which is practically the same as (54) and may be used for both model I and model II. If $L \gg a$, the integral term of (60) becomes $\sim 8\mu UL/a^2$, and we obtain from (60)

$$U = \left(P + \frac{2\gamma_L}{a}\cos\theta_d\right)a^2/8\mu L\left\{1 - \frac{a}{\pi L}(\ln\epsilon + 0{\cdot}410)\right\}, \tag{61}$$

in which we have set $-\tan(\theta_d - 90°) \simeq \cos\theta_d$ since $\theta_d \simeq 90°$. Equation (61) is written in a form similar to (59) but with a correction to L, which accounts for the presence of the meniscus. For systems in which θ_d is not close to 90°, (61) does not, of course, apply and an added correction is needed for the liquid flow near the *curved* meniscus.

Careful microscopic observations of the contact-line movement can determine which of the spreading mechanisms suggested in the introduction applies to a particular spreading system. In view of the great difficulty in performing such experiments, our complementary theoretical study of the possibility of slippage may suggest a direction for experimental observations. Future theoretical efforts should be directed at solutions to the slippage models for contact angles not close to 90° and for various geometries of the spreading interface, and at better estimates of the slip length once the spreading process is better understood from the molecular point of view.

The authors are grateful to Professor R. G. Cox for many helpful suggestions. This research was supported by the Defence Research Board of Canada (DRB grant 9530-47).

REFERENCES

Abramowitz, M. & Stegun, I. A. 1965 *Handbook of Mathematical Functions*. Dover.

Bhattarcharji, S. & Savic, P. 1965 *Proc. Heat Transfer Fluid Mech. Inst.* p. 248.

Bulkley, R. 1931 *J. Res. Nat. Bur. Stand.* **6**, 89.

Cole, J. D. 1968 *Perturbation Methods in Applied Mathematics*, Blaisdell.

Derjaguin, B. V. & Fedyakin, N. N. 1969 *Sov. Phys. Dokl.* **13**, 1053.

Dryden, H. L., Murnaghan, F. D. & Bateman, H. 1956 *Bull. Nat. Res. Counc.* no. 84. *Rep. Comm. Hydrodyn.* Dover.

Dussan V., E. B. & Davis, S. H. 1974 *J. Fluid Mech.* **65**, 71.

Elliott, G. E. P. & Riddiford, A. C. 1967 *J. Colloid Interface Sci.* **23**, 389.

Garabedian, P. R. 1966 *Comm. Pure Appl. Math.* **19**, 421.

Hansen, R. S. & Miotto, M. 1957 *J. Am. Chem. Soc.* **79**, 1765.

Hansen, R. J. & Toong, T. Y. 1971*a* *J. Colloid Interface Sci.* **36**, 410.

Hansen, R. J. & Toong, T. Y. 1971*b* *J. Colloid Interface Sci.* **37**, 196.

Hoffman, R. L. 1975 *J. Colloid Interface Sci.* **50**, 228.

Huh, C. & Scriven, L. E. 1971 *J. Colloid Interface Sci.* **35**, 85.

Inverarity, G. 1969 *Brit. Polymer J.* **1**, 245.

Miller, C. A. & Ruckenstein, E. 1974 *J. Colloid Interface Sci.* **48**, 368.

Oliver, J. F., Huh, C. & Mason, S. G. 1977 To be published.

Pearson, J. R. A. 1966 *Mechanical Principles of Polymer Melt Processing*. Pergamon.

Rose, W. & Heins, R. W. 1962 *J. Colloid Sci.* **17**, 39.

Schonhorn, H., Frisch, H. L. & Kwei, T. K. 1966 *J. Appl. Phys.* **37**, 4967.

Taber, J. J. 1969 *Soc. Pet. Eng. J.* **9**, 3.

Tolstoi, D. M. 1952*a* *Dokl. Akad. Nauk SSSR* **85**, 1089.

Tolstoi, D. M. 1952*b* *Dokl. Akad. Nauk SSSR* **85**, 1329.

Washburn, E. W. 1921 *Phys. Rev.* **17**, 273.